

Physical, Structural, and Mechanical Characterization of Calcium–Shellac Microspheres as a Carrier of Carbamide Peroxide

Jing Xue, Zhibing Zhang

Centre for Formulation Engineering, School of Chemical Engineering, University of Birmingham, Edgbaston, Birmingham B15 2TT, United Kingdom

Received 30 October 2008; accepted 21 January 2009

DOI 10.1002/app.30090

Published online 14 April 2009 in Wiley InterScience (www.interscience.wiley.com).

ABSTRACT: Calcium–shellac microspheres with encapsulated carbamide peroxide (CP) were made by emulsification to generate an emulsion including shellac ammonium salt aqueous solution with soluble CP dispersed in sunflower oil with calcium chloride powders, followed by gelation between shellac and calcium. The effects of formulation and processing conditions on the encapsulation efficiency of CP, the physical, structural, and mechanical properties of calcium–shellac microspheres, including size, inner structure, and mechanical strength, were investigated. The sizes of the prepared microspheres were in the range of 10–100 μm , depending on the agitation speed used in the emulsification process. The morphology of calcium–shellac microspheres was

characterized using scanning electron microscopy and image analysis. Their inner structure was evaluated using X-ray microcomputed tomography, and their mechanical strength was determined by a micromanipulation technique. The structure and mechanical strength of the microspheres were compared with those bigger calcium–shellac beads (1–3 mm in diameter) made by extrusion followed by gelation (Xue and Zhang, *J Microencapsul* 2008, 25, 523), and clear contrast in the properties between the two preparation methods has been found. © 2009 Wiley Periodicals, Inc. *J Appl Polym Sci* 113: 1619–1625, 2009

Key words: carbamide peroxide; gelation; mechanical strength; microencapsulation; micromanipulation; shellac

INTRODUCTION

Dental care products, especially those used for tooth whitening, have drawn more attention over the recent years. The current tooth whitening methods and products are either very expensive or not effective. There is a growing trend to incorporate tooth whitening ingredients in toothpaste or chewing gum. Carbamide peroxide (CP) is the most popular tooth whitening ingredient because of its effectiveness in tooth whitening and safety for oral use with a controlled dosage. However, CP is a strong oxidant and is incompatible with some other ingredients in toothpaste or chewing gum such as antibacterial ingredients and flavors. It is probably one of the most difficult molecules to be encapsulated. Recent work showed that calcium–shellac beads produced by an extrusion process followed by gelation may be used as a carrier of CP.¹ However, in general, the sizes of the beads produced by the extrusion–gelation process were bigger than 1 mm. For some industrial applications, it may be desirable to produce particles in the range of microns.

Shellac is a natural, biodegradable, and renewable resin of insect *Kerria lacca*.² It has the features of low water permeability and excellent film-forming properties.^{3–5} It is enteric and listed as a food additive. Conventionally, the most popular uses of shellac flakes include pharmaceutical, confectionery, and food coatings. Shellac has been used to coat intestine's pills containing ingredient, which can upset stomach, so that they will not dissolve in the stomach but in the lower intestine. It has also been used as a coating of pills to realize "time release" medication and provide protective candy coating or glazes.⁶

A process involving emulsification followed by gelation has been established to produce calcium alginate microspheres.^{7–10} In this process, insoluble calcium carbonate powders were mixed with sodium alginate solution, which was dispersed in an oil phase. Acetic acid was added to the oil phase, leading to the release of the calcium ion from calcium carbonate, which gelatinized sodium alginate to form solid calcium alginate microspheres.¹¹ Their sizes were controlled by the type and agitation speed of an impeller used to generate the emulsion. The process has been investigated to encapsulate protein,¹² hemoglobin,¹³ food ingredients for fish,¹⁴ drugs for oral delivery,¹⁵ and living cells such as yeasts for fermentation and pancreatic islets for

Correspondence to: Z. Zhang (z.zhang@bham.ac.uk).

clinical applications.^{16–18} However, the aforementioned emulsification–gelation method cannot be directly applied to produce calcium–shellac microspheres as aqueous shellac solution tends to precipitate and form tiny solid particles in acidic liquid, which can occur after acetic acid is added to the system. In this work, the emulsification–gelation method was modified by replacing calcium carbonate powders with calcium chloride (CaCl_2) powders, which were dispersed in oil phase to encapsulate water-soluble CP. The formed calcium–shellac microspheres were characterized in terms of size, morphology, structure, and mechanical strength.

MATERIALS AND METHODS

Materials

All chemicals were obtained from Sigma, UK, and used as received, with the exception of ammonium salt of shellac (Marcoat 125), which was a generous donation from Syntapharm, Harke Group, Germany. It is based on dewaxed and decolorized shellac refined in a solvent extraction process. The chemical structure of shellac is not modified by this process. This aqueous formulation has a shellac content of $25\% \pm 1\%$ (mean \pm standard error) by weight, pH of 7.3 ± 0.3 , and density of 1.04 ± 0.03 g/mL.

Methods

Preparation of calcium–shellac microspheres via emulsification followed by gelation

The schematic diagram of the emulsification–gelation process is shown in Figure 1. CP (0.75 g) was dissolved in 5 mL shellac solution. The mixture of CP and shellac was dispersed in 200 mL sunflower oil by a 45° flat-blade disk turbine impeller at an agitation speed of 200 rpm for 30 min. CaCl_2 powder (1 g) was added slowly into the water/oil (w/o) system. Agitation was maintained for another 2 h. The formed microspheres settling at the bottom of the stirred vessel were collected after the agitation was stopped, washed by 2% Tween 80 solution, and dried at room temperature ($24 \pm 1^\circ\text{C}$) for 24 h by a freeze dryer [Edward (EF03) Freeze dryer, UK].

Measurement of encapsulation and loading efficiencies of carbamide peroxide

The encapsulation efficiency (EE) and loading efficiency (LE) of CP were determined using a ceric titration method.¹ Calcium–shellac microspheres were ground into small pieces using a pestle and mortar manually. Distilled water of 4°C was added to extract CP. The concentration of hydrogen peroxide in aqueous solution was determined by titrating it

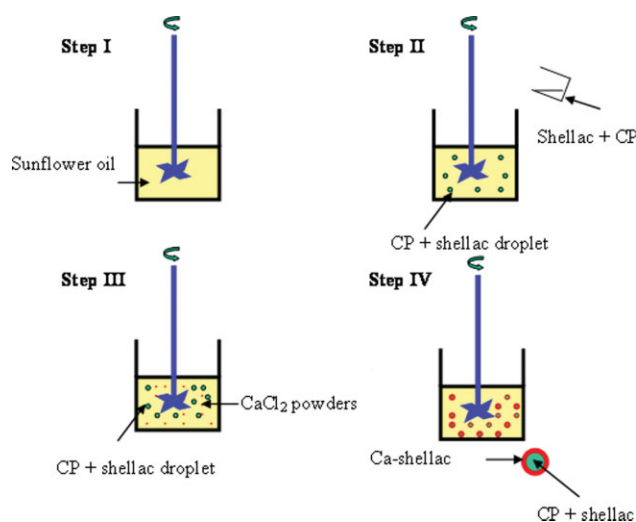


Figure 1 The schematic diagram describing encapsulation of carbamide peroxide using calcium–shellac by a process of emulsification followed by gelation. [Color figure can be viewed in the online issue, which is available at www.interscience.wiley.com.]

with standardized solution of ceric sulfate (0.1N) to a pale blue end point using ferroin as an indicator. This procedure is appropriate for characterizing 1% (wt %) to 30% (wt %) hydrogen peroxide content in either aqueous solution or mixture, which has an equivalent amount of hydrogen peroxide within this range.

Characterization of size, morphology, and inner structure of calcium–shellac microspheres

The sizes of the formed calcium–shellac microspheres after they were freeze dried were measured using an image analysis system (Quantiment Q570 Image Analyzer, Leica, UK). Their morphology was characterized using scanning electron microscopy (SEM) (Model S-2300, Hitachi, Japan). X-ray micro-computed tomography (micro-CT; Skyscan 1072, Skyscan, Belgium), which consists of a microfocus-sealed X-ray tube with a spot size of $5\ \mu\text{m}$ operating at a voltage of 100 kV and current of $96\ \mu\text{A}$, was used to obtain the inner cross-sectional image of calcium–shellac microspheres.¹

Determination of the mechanical strength of calcium–shellac microspheres

A micromanipulation technique¹⁹ was applied to measure the mechanical properties of calcium–shellac microspheres with encapsulated CP. The schematic drawing of the micromanipulation rig is shown in Figure 2. Dried microspheres that were well dispersed on a glass slide by a cotton stick were placed under the flat end of a glass probe, which was attached to the output tube of a force

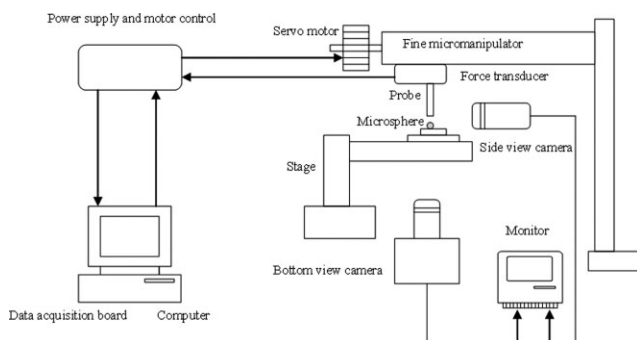


Figure 2 Schematic diagram of the micromanipulation rig.

transducer (Model 402A, Aurora Scientific, Canada) using superglue. The force transducer itself was mounted onto a three-dimensional micromanipulator, which was driven by a servo motor (Parker Compumotor, USA). A motor controller allowed the distance and speed of movement in the vertical direction to be controlled. The glass slide was fixed onto a metal stage, which was connected to a second micromanipulator. The entire compression process was observed by side-view and bottom-view microscopes, which were focused on the particle of interest. A TV monitor was connected to the microscopes to measure the size of the particle and get a clear view of the experimental process as well.

Single microspheres were compressed to rupture at a compression speed of $2 \mu\text{m/s}$. The corresponding force versus sampling time or microsphere displacement data were obtained.

RESULTS AND DISCUSSION

Encapsulation efficiency and loading efficiency

The EE of CP and its LE in calcium-shellac microspheres were determined straightly after the encapsulation process. The EE and LE are shown in Figure 3.

Figure 3 illustrates the effect of varying amount of CP input on its EE and LE. As the CP input was increased from 0.05 to 0.15 g/mL, its EE increased from $51\% \pm 2\%$ to $65\% \pm 2\%$. When the input of CP was greater than 0.15 g/mL, aggregation of calcium-shellac microspheres was observed. This result is consistent with the EE of CP in calcium-shellac beads produced by the extrusion-gelation process.¹ Corresponding to the increase of CP input from 0.05 to 0.15 g/mL, its LE increased from $3.9\% \pm 0.5\%$ to $13\% \pm 2\%$, as expected.

Morphology, size distribution, and circularity of calcium-shellac microspheres

The SEM images of calcium-shellac microspheres after freeze drying are presented in Figure 4. It can

be seen from the SEM images that calcium-shellac microspheres were still relatively spherical.

The size distribution of the freeze-dried microspheres is shown in Figure 5. The microsphere diameter varies from 13 to $70 \mu\text{m}$, and the mean diameter is $31 \pm 1 \mu\text{m}$. The mean circularity of the microspheres is 1.1 ± 0.1 (distribution data not shown), which is consistent with their SEM images.

Inner structure of calcium-shellac microspheres

The reconstructed horizontal 2D image of the central layer of calcium-shellac microspheres is presented in Figure 6. In the reconstructed 2D horizontal slice image, the black areas represent the pores and the white areas represent the dense materials.

Figure 6(A) shows the cross-sectional image of a group of freeze-dried calcium-shellac microspheres. The noise level and ring effect of the image is high due to the limitation of X-ray micro-CT, which has the resolution of $5 \mu\text{m}$ per pixel. The sizes of the microspheres in this group are close to the resolution of the X-ray micro-CT, and therefore the quality of the reconstructed image is not adequate enough to identify their inner structure of such small microspheres. To overcome this problem, a batch of calcium-shellac microspheres with the sizes over $300 \mu\text{m}$ were prepared using the same emulsification-gelation process but an agitation speed of 120 rpm and 2 mL of shellac solution with 0.15 g/mL CP input; their inner structure is shown in Figure 6(B). For comparison, the inner structure of a calcium-shellac bead made by the extrusion-gelation process¹ is shown in Figure 6(C). It can be seen from Figure 6(B,C) that the calcium-shellac microsphere

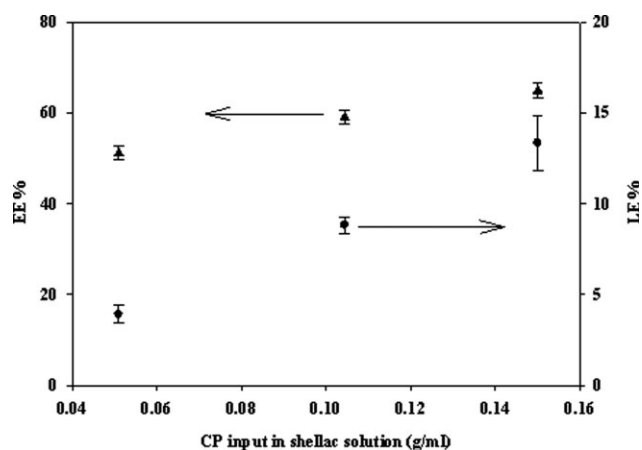


Figure 3 The effect of CP mass on its encapsulation and loading efficiencies. Five milliliter of aqueous ammonium shellac solution was used, the input of CaCl_2 powders was 1.5 g, and the agitation speed was 200 rpm. The error bars represent the interval of the measurements from two repeated experiments.

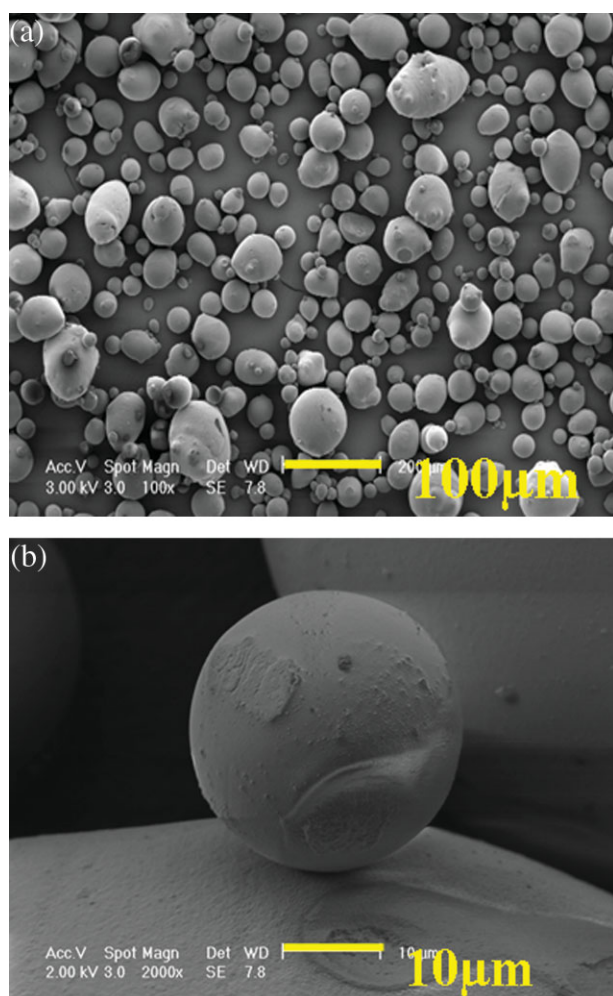


Figure 4 Images of freeze-dried calcium-shellac microspheres under SEM with different magnifications. [Color figure can be viewed in the online issue, which is available at www.interscience.wiley.com.]

made from the emulsification-gelation process had a much more condensed structure than that of the calcium-shellac bead made from the extrusion-gelation

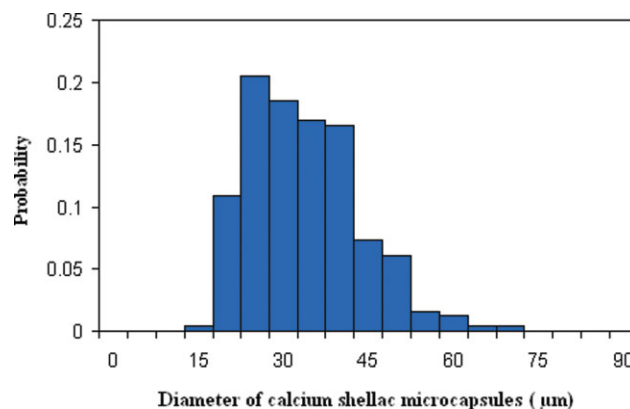


Figure 5 Size distribution of calcium-shellac microspheres, which were formed with 0.75 g CP mixed with 5 mL ammonium shellac solution. The agitation speed was 200 rpm and number of microspheres counted 307. [Color figure can be viewed in the online issue, which is available at www.interscience.wiley.com.]

process. The relative cross-sectional solid area of particles was then extracted from the reconstructed 2D horizontal slice images using T-view image software (Skyscan, 2003) and is defined as follows:

$$\text{Relative solid area (\%)} = \frac{\text{Number of active pixel (solid area) in region of interest}}{\text{Number of total pixel in region of interest}} \times 100. \quad (1)$$

The relative solid area of calcium-shellac microspheres produced by the emulsification-gelation process is $92\% \pm 7\%$ (based on images of five particles in the sample), which is significantly greater than that of those produced by the extrusion-gelation process, $30\% \pm 5\%$. The difference in relative solid area between the particles produced by the two methods may be explained as follows. When the calcium ion contacted the shellac, they reacted to form solid calcium-shellac particles,¹ which created

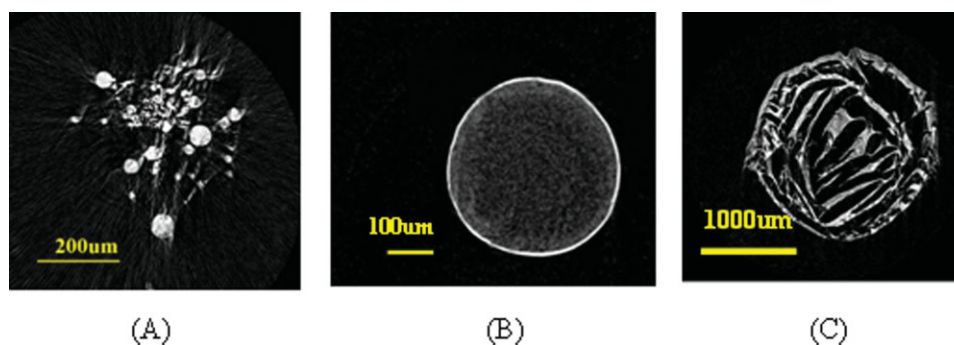


Figure 6 Reconstructed images of calcium-shellac microspheres and bead, obtained using X-ray microcomputed tomography. (A) Several freeze-dried calcium-shellac microspheres (13–60 μm in diameter). (B) A big calcium-shellac microsphere (400 μm) produced by the emulsification-gelation process with an agitation speed of 120 rpm for illustration. (C) A calcium-shellac bead (1670 μm) produced by the extrusion-gelation process¹ for comparison. [Color figure can be viewed in the online issue, which is available at www.interscience.wiley.com.]

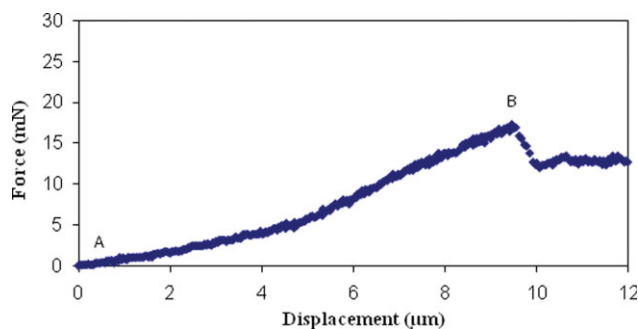


Figure 7 Typical force versus displacement relationship for compressing single calcium-shellac microsphere to rupture. The diameter of the microsphere was 40 μm . [Color figure can be viewed in the online issue, which is available at www.interscience.wiley.com.]

a barrier for mass transfer, and thus slowed down diffusion of calcium ion into the center of the particles. By comparing the microspheres made by the emulsification-gelation process and beads by extrusion-gelation,¹ the formed microspheres were much smaller and had much bigger specific surface area (area per unit volume). Consequently, it took less time for calcium ion to reach the center of the microspheres, and the amount of calcium ion across their surface should be greater for a given period of time. Moreover, the emulsification-gelation process to produce calcium-shellac microspheres was a relatively slow process, which took 2 h, in contrast with 20 min for the extrusion-gelation process. The combined effect resulted in the more compact structure and higher relative solid area of the calcium-shellac microspheres than the beads.

Rupture force and nominal rupture stress

Figure 7 shows a typical curve of force versus displacement for compression of a single calcium-shellac microsphere to rupture. Points A and B correspond to the microsphere being compressed. At Point B, the calcium-shellac microsphere was ruptured and there was a clear reduction in the force imposed on the microsphere. The force at Point B was defined as the rupture force of the calcium-shellac microsphere. The nominal rupture stress of the microsphere was determined by the ratio of the rupture force to initial cross-sectional area,²⁰ and the nominal deformation at rupture by the ratio of the displacement at rupture to initial diameter.

The rupture force of calcium-shellac microspheres increases with diameter on average [Fig. 8(A)], which is consistent with the results obtained before on other types of particles, e.g., melamine formaldehyde microcapsules.¹⁹ This trend is in contrast with that of the calcium-shellac beads produced by the extrusion-gelation process where the rupture force

decreased with diameter.¹ The contrast might result from that the calcium-shellac beads produced by the extrusion-gelation process had a less condensed structure than the calcium-shellac microspheres produced by the emulsification-gelation process, as shown in Figure 6(B,C). The nominal rupture stress decreases with the diameter [Fig. 8(B)], which is expected and indicates that bigger particles were weaker and tended to be broken more easily at end-use applications, e.g., in chewing gum or tooth

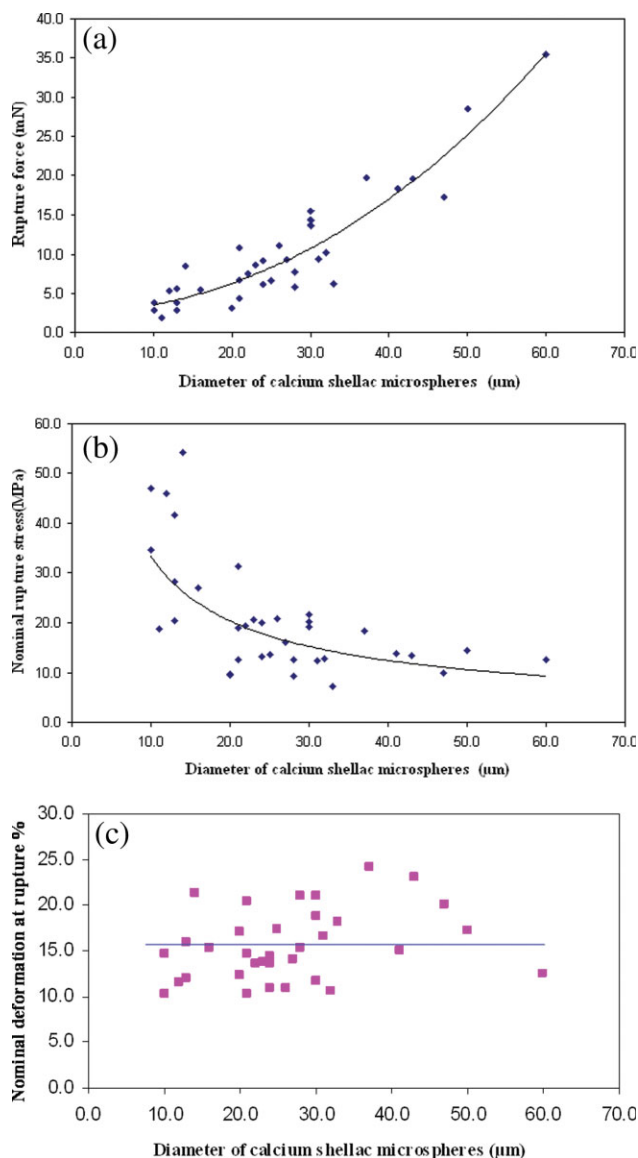


Figure 8 Mechanical property data obtained from micro-manipulation measurements of single calcium-shellac microspheres. (A) Rupture force versus diameter of calcium-shellac microspheres. (B) Nominal rupture stress versus diameter. (C) Nominal deformation at rupture versus diameter. This batch of calcium-shellac microspheres was produced with an agitation speed of 200 rpm. The solid lines only indicate the trends. [Color figure can be viewed in the online issue, which is available at www.interscience.wiley.com.]

paste. In Figure 8(C), it can be seen that the nominal deformation at rupture does not seem to vary with diameter, and the mean value is $16\% \pm 1\%$.

The mean values of rupture force, nominal rupture stress, and deformation at rupture of the microspheres are summarized in Table I, in comparison with those of calcium-shellac beads produced by the extrusion-gelation process.¹

As it can be seen from Table I, the mean nominal rupture stress of calcium-shellac microspheres is 21 ± 2 MPa, which is much greater than that produced by the extrusion process, 0.07 ± 0.01 MPa. This result is consistent with Figure 6(B,C) as the calcium-shellac beads produced by the emulsification-gelation process were much smaller and more compact than the beads produced by the extrusion-gelation process.

Young's modulus

Suppose single elastic particles are compressed between two parallel surfaces and the deformation is small (e.g., less than 10%), the force (F) – displacement (δ) relationship may be described by Hertz model²¹ as follows:

$$F = \frac{4}{3} \frac{E}{(1 - \nu^2)} R^{1/2} \left(\frac{\delta}{2} \right)^{3/2}, \quad (2)$$

where E is the Young's modulus of the particle, ν is the Poisson's ratio, and R is the initial particle radius.

The Hertz model [eq. (2)] was applied to fit the force versus displacement data of compressing calcium-shellac microspheres to a nominal deformation of 10% in Figure 7. The force versus displacement data fitted with the Hertz model is shown in Figure 9. As can be seen, there is a very good agreement between them with a correlation coefficient of 0.97. From eq. (2), the Young's modulus of this micro-

TABLE I
Comparison of the Mechanical Property Parameters of Calcium-Shellac Microspheres Prepared by the Emulsification-Gelation Process and the Beads by the Extrusion-Gelation Process

	Calcium shellac microspheres produced by emulsification	Calcium shellac beads produced by extrusion ^{1,22}
Diameter (μm)	31 ± 1	1904 ± 32
Rupture force (mN)	10 ± 1	191 ± 23
Nominal rupture stress (MPa)	21 ± 2	0.07 ± 0.01
Deformation at rupture (%)	16 ± 1	5.4 ± 0.7
Number of particles compressed	35	30

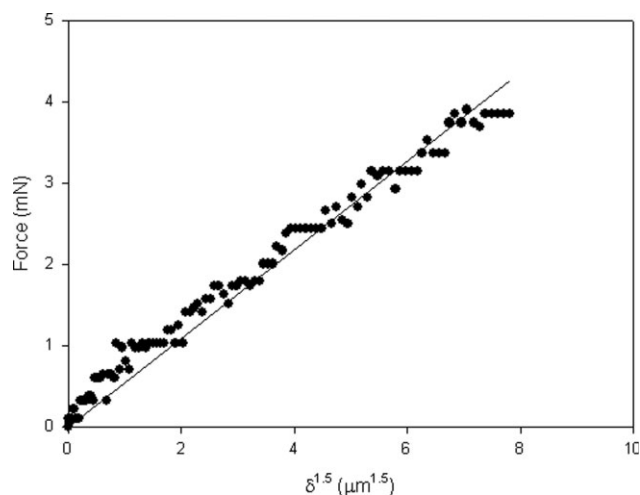


Figure 9 The linear fit of the Hertz model to the loading data of compressing a single calcium-shellac microsphere to a final nominal deformation of 10% (diameter $40 \mu\text{m}$). The compression speed was $2 \mu\text{m/s}$.

sphere was determined assuming the material was incompressible (i.e., $\nu = 0.5$).

The mean value of Young's modulus of calcium-shellac microspheres was calculated to be 533 ± 92 MPa, whereas the mean value of calcium-shellac beads made from the extrusion process was only 0.28 ± 0.03 MPa.²² These results are consistent with the structural features of the microspheres and beads, as shown in Figure 6.

CONCLUSIONS

The work showed that calcium-shellac microspheres in the size range of $10\text{--}100 \mu\text{m}$ have been successfully produced by the emulsification-gelation process. CP was encapsulated by calcium-shellac microspheres using this method. The EE of CP was determined to be in the range of $51\text{--}65\%$, which is similar to that obtained by the extrusion-gelation process reported earlier. The calcium-shellac microspheres made by the emulsification-gelation process had a condensed structure and no big pore was observed from their cross-sectional area.

The experimental results obtained using micromanipulation showed that the rupture force of the calcium-shellac microspheres on average increased with diameter, whereas the nominal rupture stress decreased with diameter. The mean nominal rupture stress of shellac microspheres was much greater than that of calcium-shellac beads made by the extrusion-gelation process. This might be due to the bigger size and higher porosity of the latter.

The Hertz model [eq. (2)] was used to fit the experimental data of force versus displacement obtained from compressing single calcium-shellac microspheres to a final nominal deformation of 10%.

The mean Young's modulus of calcium-shellac microspheres was found to be 533 ± 92 MPa.

The results demonstrate that the size, structure, and mechanical strength of calcium-shellac particles as a carrier of CP can be tailored using different preparation methods to meet various requirements of industrial applications. It is believed that calcium-shellac particles can also be used to encapsulate other aqueous-based active ingredients, which will be investigated in future.

References

1. Xue, J.; Zhang, Z. *J Microencapsul* 2008, 25, 523.
2. Cockeram, H. S.; Levine, S. A. *J Soc Cosmet Chemists* 1961, 12, 316.
3. Sheorey, D. S.; Shastri, A. S.; Dorle, A. K. *Int J Pharm* 1991, 68, 19.
4. Nadian, A.; Lindblom, L. *Int J Pharm* 2002, 242, 63.
5. Pearnchob, N.; Dashevsky, A.; Bodmeier, R. *J Controlled Release* 2004, 94, 313.
6. Jewitt, J. *Hand-Applied Finishes*, Taunton Press, 1997.
7. Poncelet, D.; Poncelet De Smet, B.; Beaulieu, C.; Huguet, M. L.; Fournier, A.; Neufeld, R. *J Appl Microbiol Biotechnol* 1995, 43, 644.
8. Chan, L. W.; Heng, P. W. S.; Wan, L. S. C. *J Microencapsul* 1997, 14, 5.
9. Poncelet, D. *Ann NY Acad Sci* 2001, 944, 74.
10. Liu, X. D.; Yu, W. T.; Lin, J. Z.; Ma, X. J.; Yuan, Q. *Chem Res Chin Univ* 2007, 23, 579.
11. Poncelet, D.; Babak, V.; Dulieu, C.; Picot, A. *Colloids Surf A* 1998, 155, 171.
12. Silva, C. M.; Ribeiro, A. J.; Figueiredo, I. V.; Goncalves, A. R.; Veiga, F. *Int J Pharm* 2006, 311, 1.
13. Ribeiro, A. J.; Silva, C.; Ferreira, D.; Veiga, F. *Eur J Pharm Sci* 2005, 25, 31.
14. Yúfera, M.; Fernández-Díaz, C.; Pascual, E. *Aquaculture* 2005, 248, 253.
15. Rastogi, R.; Sultana, Y.; Aqil, M.; Ali, A.; Kumar, S.; Chuttani, K.; Mishra, A. K. *Int J Pharm* 2007, 334, 71.
16. Tze, W. J.; Cheung, S. C.; Tai, J.; Ye, H. *Transplant Proc* 1998, 30, 477.
17. Najafpour, G.; Younesi, H.; Syahidah, K. I. K. *Bioresour Technol* 2004, 92, 251.
18. Chan, L. W.; Lee, H. Y.; Heng, W. S. *Carbohydr Polym* 2006, 63, 176.
19. Sun, G.; Zhang, Z. *J Microencapsul* 2001, 18, 593.
20. Yap, S. F.; Adams, M. A.; Seville, J. P. K.; Zhang, Z. *China Particuology* 2006, 4, 35.
21. Hertz, H. *Miscellaneous Pap* 1896, 92, 156.
22. Xue, J. Ph.D. Thesis, University of Birmingham, Birmingham, UK, 2008.